

Non-radial Pulsation Modeling of μ Centauri

Th. Rivinius

Landessternwarte Königstuhl, D-69117 Heidelberg, Germany

Abstract. It is shown that the line profile variability (*lpv*) of μ Cen can be modeled as non-radial pulsations (*nrp*). The use of the most recent available modeling technique for the *nrp* and carefully computed stellar observables (intrinsic line profile and flux) are, however, mandatory to take full advantage of present high-quality data.

1. Introduction

The most natural explanation for the observed multiperiodic properties of μ Cen (Rivinius et al., 1998, and Baade et al., this volume) is nonradial pulsation (*nrp*). However, a mode identification by means of accurate physical modeling is still to be obtained. Townsend's (1997) modeling codes BRUCE and KYLIE are used to investigate the periodic variability. BRUCE calculates the pulsational disturbances of a rotating stellar surface (including gravity darkening).

The input for BRUCE are the stellar parameters, the angular pulsational indices, and amplitude for each mode. The statically rotating stellar model is perturbed by: i) pulsational velocity field that is superimposed on the rotation, ii) temperature and $\log g$ perturbations, iii) variations of the visible area, and iv) deviations of the local surface normal vector from the radial direction.

KYLIE then integrates observables from the surface structure computed by BRUCE. This requires an input grid containing information about the undisturbed intrinsic observables of a stellar surface element depending on temperature, gravity, wavelength, and viewing angle. The variability due to deviations of the local surface normal vector, $\cos \mu$, was not treated by earlier models and enables to estimate the photometric variability due to a given mode. The input grid contains intrinsic (local) line profiles for estimating the line profile variability, while for photometry estimates the flux emerging from a standard surface element under different conditions is needed.

2. Synthetic Fluxes and Line Profiles

Kurucz's ATLAS 9 code was used to compute the atmospheric fluxes from 10 000 to 30 000 K and $\log g$ from the lowest converging value to 4.5. This grid is, however, not able to cover the variability due to variations in aspect angle on a given surface element. The treatment of limb darkening is therefore crucial. Parameterized linear limb darkening coefficients for the standard photometric bands were used (Díaz-Cordovés et al. 1995). ATLAS 9 also gives the atmospheric

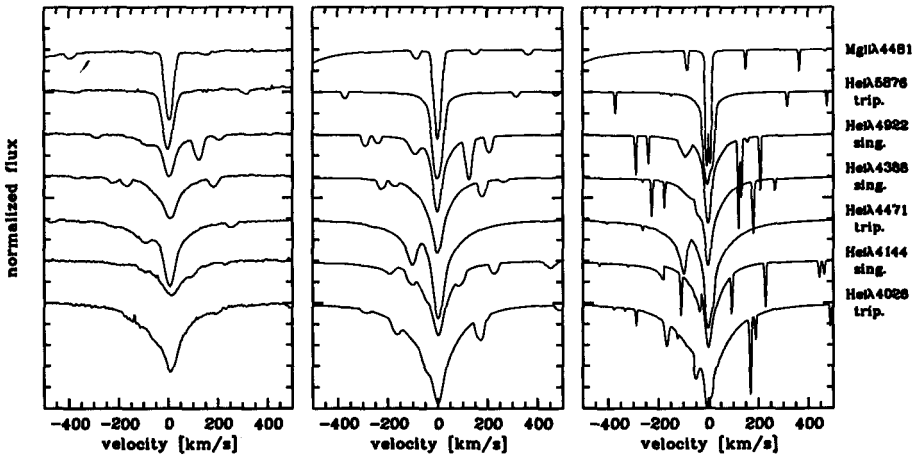


Figure 1. Left: He I lines of HR 4206, middle: Synthetic spectrum broadened with $v \sin i = 20$ km/s, right: unbroadened synthetic spectrum ($T_{\text{eff}} = 16\,000$ K, $\log g = 3.5$). The line identifications are given on the right side. Note that, independent of their singlet/triplet nature, only few of the He I lines might be approximated by a Gaussian. However, even those and the metal lines should be computed explicitly because of the $T_{\text{eff}} - \log g$ dependence (cf. Sect. 2)

structure needed as input to model the intrinsic line profiles. For the computed atmosphere structures an LTE line profile grid has been calculated using the BHT-code by Baschek et al. (1966). For a more detailed description of the atmospheric modeling see Gummersbach et al. (1998).

BHT puts special emphasis on the treatment of the helium spectrum. This is demonstrated in Fig. 1, where the model results are compared to a spectrum of HR 4206, which was classified as a Be star but appears as non-emission single-, narrow-lined spectroscopic binary in our data. Note that also for metallic lines the intrinsic line width is not treated as free parameter, but in the framework of the used line formation theory given by temperature, $\log g$ and microturbulence, which was fixed at $\xi_{\text{micro}} = 2$ km/s.

Even for the same ionization stage of a given atom various spectral lines may behave in a different way in T_{eff} and $\log g$. This partly explains the observed differences between spectral lines of He I and again emphasizes the importance of using adequately computed input data instead of parameterized intrinsic profiles.

3. Non-radial Pulsation Modeling

For the pulsationally undisturbed star, a polar radius of $5.8 R_{\odot}$, a polar temperature of $22\,000$ K, a mass of $8 M_{\odot}$, an equatorial rotation of 200 km/s, and an inclination of 40° were adopted, being acceptable for a B2.5 IV-V star. For this single set of stellar parameters the properties of all periods in the investigated spectral lines could be modeled simultaneously. Two examples of He I lines are

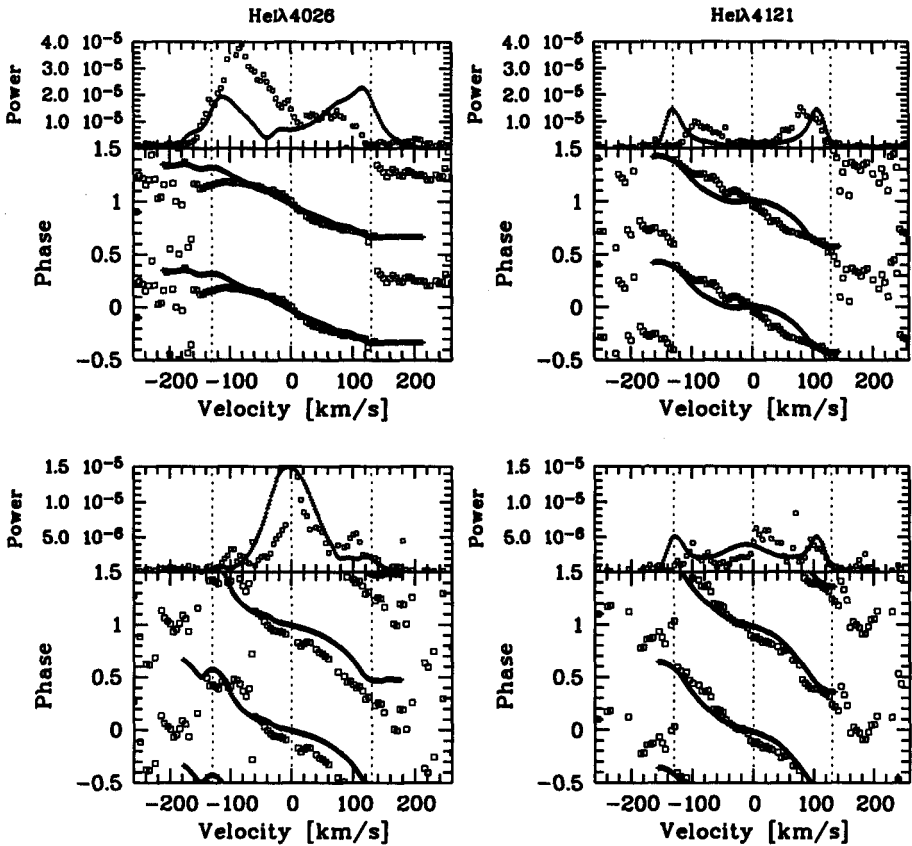


Figure 2. Data (\square) for \mathcal{P}_1 (upper row) and \mathcal{P}_5 (lower row) compared to the model ($+$) in terms of a 2D-frequency analysis across the profile

presented in Fig. 2. The main modes of either period group of identical appearance (Rivinius et al., 1998), $\mathcal{P}_1=0.5029$ and $\mathcal{P}_5=0.2814$ day, have been modeled by now. We show examples for $l = 2, m = -1$ (\mathcal{P}_1) and $l = 3, m = -2$ (\mathcal{P}_5). While the appearance changes drastically with m , l may vary by ± 1 without degrading the agreement to much. Besides the generally good agreement, the differences between spectral lines are reproduced, too. I.e. the enhanced (suppressed) power in the line center of He I 4026 (He I 4121), compared to the power in the line wings for \mathcal{P}_5 is modeled well.

Furthermore, the estimated photometric amplitude undergoes a cancellation for realistic parameter sets. Consequently, even if temperature variations are present on the star, an observed zero photometric amplitude (e.g. Cuyper et al. 1989) with the spectroscopic derived periods does not contradict nrp (Fig. 3).

However, by now it was not possible to resolve an ambiguity of the mode identification for the longer period group. Similar to 28 (ω) CMa, it could actually be a retrograde mode of similar degree that appears prograde due to

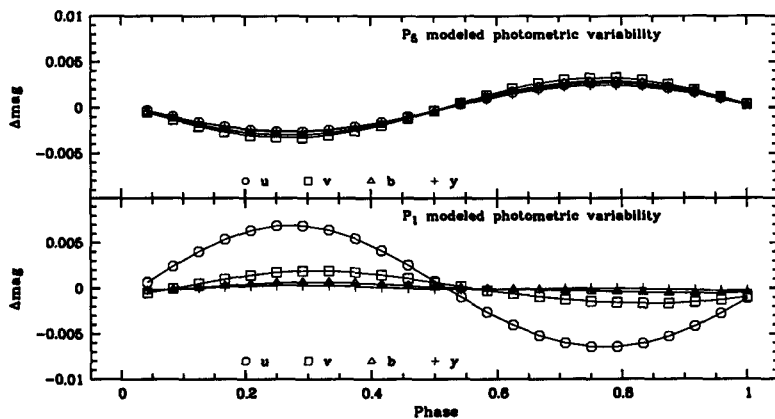


Figure 3. Modeled photometric variability for \mathcal{P}_1 and \mathcal{P}_5 in the Strömgren bands. Aerts (this volume) reports the detection of an alias of the beat frequency of \mathcal{P}_1 and \mathcal{P}_5 in photometric Hipparcos data with an amplitude of about 20 mmag. The Hipparcos sampling is however not ideally suited to recover short periods unambiguously

rapid rotation. The spectroscopic signature would, in HEROS data (Štefl and Rivinius, this volume), be indistinguishable. Data with higher resolution and S/N ratio will reveal the necessary details like backward traveling bumps, ramps, and spikes good enough to address this question (cf. Maintz et al., this volume for observed and modeled examples of such features). The stellar parameters for the retrograde solution would, however, be different.

4. Conclusions

\mathcal{P}_1 and \mathcal{P}_5 could be modeled with the same stellar parameters in good agreement with the data. However, for the longer period group an ambiguity between prograde modes or retrograde ones coupled with very rapid rotation remains and will be solved only with the help of better data. Very low or even zero amplitude light variations with the spectroscopic period in a Be star do not enforce zero-amplitude in temperature variability.

References

- Balona L.A., Aerts, C., Štefl, S. 1999, MNRAS 305, 519
 Baschek, B., Holweger, H., Traving, G. 1966, Abh. d. Hamb. Sternw. 8-1, 26
 Cuypers, J, Balona, L.A., Marang, F. 1989, A&AS 81,151
 Díaz-Cordovés, J., Claret, A., Giménez, A. 1995, A&AS 110, 329
 Gummersbach, C.A., Kaufer, A., Schäfer, D.R., et al. 1998, A&A 338, 881
 Rivinius, Th., Baade, D., Štefl, S., et al. 1998, A&A 336, 177
 Townsend, R.H.D. 1997, MNRAS 284, 839